

# Nonlinear Control of Unicycle-like Robots for Person Following

Daniele Pucci<sup>1</sup> and Luca Marchetti<sup>2</sup> and Pascal Morin<sup>3</sup>

**Abstract**—This paper addresses the person following problem for nonholonomic wheeled robots. Because of the robot's nonholonomy and the difficulty to estimate the person orientation, classical control laws used to address this problem induce strong limitations on the desired robot location with respect to the person. We propose a new nonlinear control law that allows for much more versatility in this following application. Simulation and experimental results performed in real scenarios verify the effectiveness of the proposed approach.

## I. INTRODUCTION

Developing a mobile robot that can follow a user is not a new problem in robotics [1]. Several applications can be considered, e.g. robotic shopping carts, robotic butlers that may help for carrying heavy objects, or walking-aid systems. For such mobile platforms to work properly, two basic issues must be dealt with. The first one concerns the detection of the user and the estimation of its position with respect to the robot. The second issue is the design of feedback control laws that maintain a desired relative position between the robot and the user. The following provides a short review of existing solutions to these two issues.

*People Position Estimation* is a well-known problem addressed in many scenarios such as video-surveillance [2] and activity recognition [3]. Estimating the position of the human body is complexified by several issues like the diversity of human shapes and sizes, or the number of persons in the environment. Recently, improvements in RGB-D sensor technology have made it possible to perceive 3D structures, and extended possibilities in image-based person recognition. Using the approach described in [4], for example, it is possible to recognize the person in different postures. For mobile robotic applications, a *laser range finder* is often employed to map the surrounding environment [5]. Its high precision allows one to detect obstacles and objects accurately. The information from the laser can also be used to detect and track the legs of several people [6]. Thanks to the large field of view, range, and high resolution of the sensor, the user position can be estimated with high accuracy. By exploiting the strengths of *laser range finders* and *RGB-D sensors*, one can improve the estimation of the user position [7], [8], [9].

*Robot control and person following* consist in using state measurements and estimates to stabilize the robot about a given trajectory. Feedback control of unicycle-like robots has received much attention from the scientific community

in the last decades, and many solutions to several control tasks have been proposed (See, e.g., [10] for a survey). The main difficulty comes from kinematic constraints that forbid instantaneous motion in the lateral direction of the robot.

*Person following* with a mobile robot can be viewed as a particular application of the general robot control problem. It presents, however, specific characteristics that need to be addressed properly. In particular, because of the difficulty in measuring/estimating a person's orientation, control laws can only use position measurements of the person with respect to the robot. Therefore, the proposed solutions inherit classical limitations of position control of mobile robots, like the fact that the person must be located in front of the robot so as to ensure a stable behavior of the robot's orientation. Sidenbladh et al [11] is among the first to address the robot control in the context of person following. The authors describe a mobile robot that tracks a person using a camera mounted on a pan/tilt unit. The robot control relies on a simple proportional controller to keep the image of the person centered in the camera frame. In [12], the authors present another interesting platform for person following. Focusing on person recognition, they describe a system involving a 3D lidar and a color camera. By combining information from both sensors, person tracking is achieved even in the presence of occlusions. The control algorithm is not described in details and it seems to be based on a proportional controller.

This paper presents a novel solution to the problem of person following. It is well known that position controllers typically used to solve this problem work well when the user is located in front of the robot and moves forward. In particular, the so-called *jack-knife effect* is problematic if the user starts moving backward. Feedback control laws in both position and orientation could be used to avoid this problem, but the difficulty to estimate the orientation of the user is a major issue for the implementation of these control laws. The solution proposed in this paper allows us to stabilize the robot w.r.t. the person with the latter located sideways – i.e. along the wheels' axis – and also ensures *jack-knife effect* avoidance. It can be implemented with conventional sensor suite since the control law is position-based, i.e. the relative orientation of the person w.r.t. the robot is not needed to compute the control law.

The paper is organized as follows. Section II provides background and notation. The main control results are presented in Section III. Validations of the approach are presented in Section IV, first through simulations, and then through experiments performed with a unicycle-like robot. Remarks and perspectives conclude the paper.

<sup>1</sup>Department of Robotics, Brain and Cognitive Sciences, Istituto Italiano di Tecnologia Daniele.Pucci@iit.it

<sup>2</sup>INRIA Sophia Antipolis Méditerranée, France luca.marchetti@inria.fr

<sup>3</sup>ISIR-UPMC, Paris, France morin@isir.upmc.fr This author has been supported by the "Chaire d'excellence en Robotique RTE-UPMC".

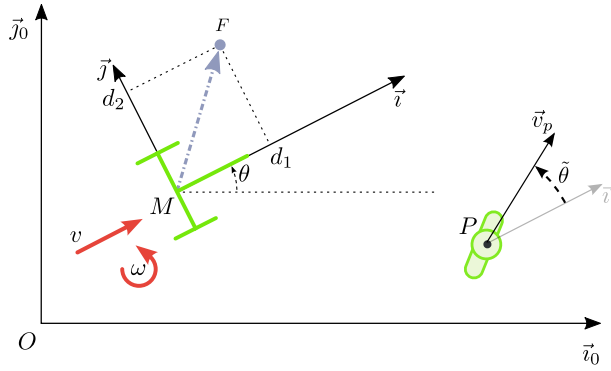


Fig. 1: Notation.

## II. BACKGROUND

### A. Notation and robot's kinematics

Consider the differential wheeled robot depicted on Figure 1. The following notation is used.

- The  $i_{th}$  component of a vector  $x$  is denoted as  $x_i$  and, for the sake of brevity,  $x_1\vec{u}+x_2\vec{w}$  is written as  $(\vec{u}, \vec{w})x$ .
- $\mathcal{I} = \{O; \vec{i}_0, \vec{j}_0\}$  is a fixed inertial frame with respect to (w.r.t.) which the robot's absolute pose is measured.
- The point  $M$  is the middle point of the wheel's axis, and  $\mathcal{B} = \{M; \vec{i}, \vec{j}\}$  is a frame attached to the robot. The vector  $\vec{i}$  is perpendicular to the wheel's axis.
- The position of the robot is given by the geometric vector  $O\vec{M}$  whose coordinates w.r.t. the inertial frame are defined by  $O\vec{M} = (\vec{i}_0, \vec{j}_0)x$ .
- $F$  denotes a point attached to the robot. Then,  $O\vec{F} = (\vec{i}_0, \vec{j}_0)x_f$  and  $M\vec{F} = (\vec{i}, \vec{j})d$ , with  $d$  a constant vector.
- The point  $P$  represents the position of a person. Then,  $O\vec{P} = (\vec{i}_0, \vec{j}_0)x_p$  and the velocity of the person is defined by  $\vec{v}_p := \frac{d}{dt}O\vec{P} = (\vec{i}_0, \vec{j}_0)\dot{x}_p$ .
- $e_1 := (1, 0)^T$  and  $e_2 := (0, 1)^T$  denote the canonical basis vectors of  $\mathbb{R}^2$ .
- The rotation matrix of an angle  $\theta$  is denoted as  $R(\theta)$ ;  $S = R(\pi/2)$  is the unitary skew-symmetric matrix, i.e.

$$R(\theta) = \begin{pmatrix} \cos \theta & -\sin \theta \\ \sin \theta & \cos \theta \end{pmatrix}, \quad S = \begin{pmatrix} 0 & -1 \\ 1 & 0 \end{pmatrix}.$$

In light of the above notation, the kinematic model of the robot writes

$$\dot{x} = vR(\theta)e_1, \quad (1a)$$

$$\dot{\theta} = \omega, \quad (1b)$$

with  $v$  and  $\omega$  the robot's rolling and rotational velocity, respectively. The variables  $v$  and  $\omega$  are considered as kinematic control inputs.

### B. Problem statement and related control issues

The control objective is to asymptotically stabilize the point  $F$  about the point  $P$ . For this purpose, define the coordinates of the geometric position error  $F\vec{P}$  as follows

$$F\vec{P} = (\vec{i}_0, \vec{j}_0)\tilde{x} = (\vec{i}, \vec{j})\tilde{p},$$

so that

$$\tilde{x} := x_f - x_p, \quad (2)$$

$$\tilde{p} := R(\theta)^T \tilde{x}. \quad (3)$$

Then, the control objective is equivalent to the asymptotic stabilization of  $\tilde{p}$  to zero. Since

$$x_f = x + R(\theta)d,$$

then differentiating Eq. (3) and using (1a) yields

$$\dot{\tilde{p}} = -\omega S\tilde{p} + Mu - v_p, \quad (4)$$

with

$$M := \begin{bmatrix} 1 & -d_2 \\ 0 & d_1 \end{bmatrix}, \quad u := \begin{bmatrix} v \\ \omega \end{bmatrix}, \quad v_p := R(\theta)^T \dot{x}_p.$$

Classical control laws that asymptotically stabilize  $\tilde{p} = 0$  when the point  $F$  is not along the wheels' axis, i.e.  $d_1 \neq 0$ , are recalled next (See e.g. [10, Sec. 34.3], [13]).

**Lemma 1** Assume that  $d_1 \neq 0$  so that  $\det(M) \neq 0$ . Apply the control input

$$u = M^{-1}[v_p - K\tilde{p}], \quad (5)$$

to System (4) with

$$K = \begin{bmatrix} k_1 & 0 \\ 0 & k_2 \end{bmatrix}, \quad K > 0.$$

Then,

$$\dot{\tilde{p}} = -\omega S\tilde{p} - K\tilde{p}, \quad (6)$$

and  $\tilde{p} = 0$  is a globally asymptotically stable equilibrium point for the closed-loop system.

This result ensures that when the control point  $F$  is not located on the wheels' axle, its stabilization to an arbitrary reference position  $P$  can be achieved by the use of simple feedback laws. This control strategy works very well when  $F$  is located ahead of the wheels' axle, which corresponds to the situation where the robot follows the user. Several limitations of this approach, however, must be mentioned. For instance, the control law is not defined when  $F$  is located on the wheel's axle and this gives rise to ill-conditioning problems when  $F$  is close to this axle (the matrix  $M$  is close to singular). Still, this situation is of practical interest for many applications where the user wants to remain close to the platform and keep it in his/her field of view. Another drawback of the control (5) is that when the robot is located behind the user, it tends to turn back if the user starts moving backward – this is the so-called *jack-knife effect*. We present below a new feedback control law to address these problems when  $F$  is located on the wheels' axle.

### III. MAIN THEORETICAL RESULTS

Assume that the point  $F$  is located on the wheels' axle, i.e.  $d_1 = 0$ . Then, System (4) writes

$$\dot{\tilde{p}} = -\omega S\tilde{p} + (v - d_2\omega)e_1 - v_p. \quad (7)$$

Eq. (7) indicates that the equilibrium condition  $\tilde{p} \equiv 0$  implies

$$T e_1 \equiv v_p \iff T R e_1 \equiv \dot{x}_p,$$

with  $T := v - d_2\omega$ . The above equation means that the robot's axis  $\iota := R e_1$  must be parallel to the velocity of the person  $\dot{x}_p$ . The control strategy then basically consists in aligning the robot's axis  $\iota$  with the velocity of the person  $\dot{x}_p$  (orientation control via  $\omega$ ) and in opposing the magnitude of  $T$  to the person's speed  $|\dot{x}_p|$  (velocity control via  $v$ ). More precisely, define  $\tilde{\theta}$  as the angle between the robot's axis  $\iota$  and the person's velocity  $\dot{x}_p$  so that (see Figure 1)

$$v_p = |\dot{x}_p| \begin{bmatrix} \cos(\tilde{\theta}) \\ \sin(\tilde{\theta}) \end{bmatrix}. \quad (8)$$

Then, the control objective  $\tilde{p} \equiv 0$  is equivalent to the asymptotic stabilization of either  $(\tilde{p}, \tilde{\theta}) = (0, 0)$  or  $(\tilde{p}, \tilde{\theta}) = (0, \pi)$ , which are associated with either  $T = |\dot{x}_p|$  or  $T = -|\dot{x}_p|$ , respectively. Now, to deal with the aforementioned *jack-knife effect*, we want these equilibria to be both stable. In this case, in fact, the angle between the robot's axis  $\iota$  and the person's velocity  $\dot{x}_p$  can be either  $\tilde{\theta} = 0$  or  $\tilde{\theta} = \pi$  (see Figure 1), so the robot is not expected to turn round when the person's velocity changes abruptly w.r.t. the robot's axis  $\iota$ . Control laws that ensure large domains of attractions for both equilibria  $(\tilde{p}, \tilde{\theta}) = (0, 0)$  and  $(\tilde{p}, \tilde{\theta}) = (0, \pi)$  are stated next.

**Theorem 1** Assume that  $\dot{x}_p(t)$  is bounded and differentiable, and that  $|\dot{x}_p(t)| \neq 0 \forall t$ . Apply the control law:

$$\begin{cases} \omega &= k_3 |\dot{x}_p|^2 \frac{v_{p2}}{v_{p1}^3} - \frac{\dot{x}_p^T S \dot{x}_p}{|\dot{x}_p|^2} - k_2 |\dot{x}_p|^2 \frac{\tilde{p}_2}{v_{p1}} \\ v &= v_{p1} - k_1 \tilde{p}_1 + d_2 \omega, \end{cases} \quad (9)$$

to System (7). Then:

- 1) the equilibrium point  $(\tilde{p}, \tilde{\theta}) = (0, 0)$  is asymptotically stable with domain of attraction equal to  $\mathbb{R}^2 \times (-\frac{\pi}{2}, \frac{\pi}{2})$ ;
- 2) the equilibrium point  $(\tilde{p}, \tilde{\theta}) = (0, \pi)$  is asymptotically stable with domain of attraction equal to  $\mathbb{R}^2 \times (\frac{\pi}{2}, \frac{3\pi}{2})$ .

The proof is given in Appendix A. Since  $v_{p1} = |\dot{x}_p| \cos(\tilde{\theta})$ , the control law (9) is singular at  $|\dot{x}_p| = 0$ , i.e. when the person does not move, and at  $\cos(\tilde{\theta}) = 0$ , i.e. when the person starts moving along the wheels' axis. Clearly, these situations may occur in practice, so desingularizing the control law (9) is imperative. In addition, note also that this law uses the person acceleration  $\ddot{x}_p$ , the estimation of which can be difficult in practice. In order to avoid these problems, we modify the control law (9) as follows

$$\begin{cases} \omega &= k_3 |\dot{x}_p|^2 \frac{v_{p2} v_{p1}}{v_{p1}^4 + \varepsilon} - k_2 |\dot{x}_p|^2 \frac{\tilde{p}_2 v_{p1}}{v_{p1}^2 + \varepsilon} \\ v &= v_{p1} - k_1 \tilde{p}_1 + d_2 \omega, \end{cases} \quad (10)$$

with  $\varepsilon$  a positive constant. Applying the control law (10) to System (7) ensures the following two properties:

- i) if  $\varepsilon = 0$  and the person's velocity is constant and different from zero, then the conclusions of Theorem 1 hold;
- ii) if the person does not move, then  $\tilde{p}$  is bounded and  $\tilde{p}_1$  tends to zero.

These properties mean that the robot's control tries to maintain the person along the wheels' axis, although the distance between the robot and the person along this axis is not guaranteed to converge to the desired value. This latter objective is achieved as soon as the person starts moving with (almost) constant velocity and  $\varepsilon$  is set equal to zero. Asymptotic stability for constant (and non zero) velocity of the person when  $\varepsilon = 0$  is sufficient to ensure practical stability and *good* tracking quality if this velocity varies "slowly" with time, and  $\varepsilon$  is relatively *small*.

The property i) of the control law (10) follows from the fact that the laws (9) and (10) coincide with  $\varepsilon = 0$  and  $\ddot{x}_p = 0$ . The property ii) can be verified by considering the following positive-definite function

$$V = |\tilde{p}|^2 / 2,$$

whose time derivative along the solutions of System (7) with the control inputs given by (10) at  $|\dot{x}_p| = 0$  is

$$\dot{V} = -k_1 \tilde{p}_1^2.$$

Since  $\dot{V}$  is negative-semi definite, then  $\tilde{p}$  is bounded. By verifying that  $\dot{V}$  is bounded, one shows that  $\tilde{p}_1$  tends to zero.

### IV. SIMULATIONS AND EXPERIMENTAL RESULTS

We tested the control law (10) by using first a simulated robot, and then a real wheeled platform – developed at INRIA Sophia Antipolis – equipped with a 2D laser finder and a 3D RGB-D camera (a Kinect). The implementation relied on the framework described in our prior work [13]. In particular, the velocity of the person is estimated from the measurement of its position under the assumption of *constant person velocity*, and the software architecture (see Figure 2) is composed of three basic modules: *Hardware Abstraction Layer*, *People Position Estimation*, and *Trajectory*

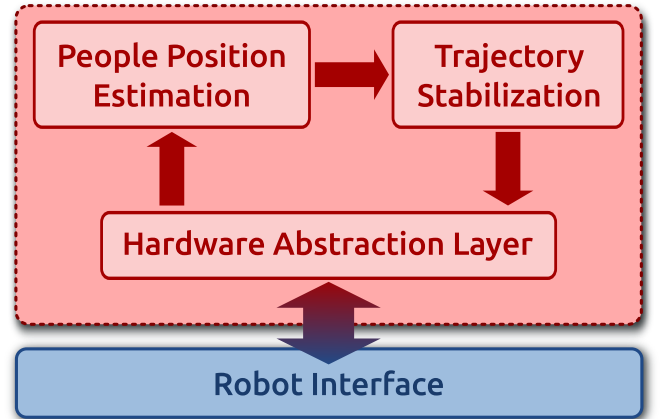


Fig. 2: Software architecture used to carry out simulations and experimental validations of the proposed control laws.

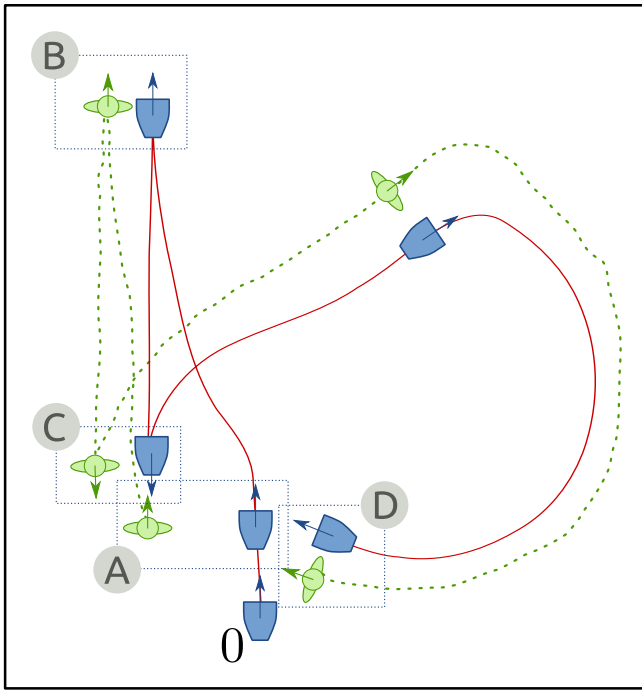


Fig. 3: Person and robot trajectories.

*Stabilization.* The first module interfaces the robot, either real or simulated, to the upper level. The *People Position Estimation* module is responsible for *fusing* the (person) position measurements from a 2D laser range finder and a 3D RGB-D camera. These measurements are used in a multi-sensor particle filter, the outcome of which is an estimation of the position of the person that must be followed by the robot. The *Trajectory Stabilization* module takes this position estimation as input in order to compute the control law (10). The reader is referred to [13] for more details on software architecture and data fusion algorithm.

Prior to experimental validations, we tested our control strategy through simulations carried out by using the robotic simulator Stage. Standard localization packages provided by ROS (amcl) were used. The simulated robot included a Hokuyo-like laser range finder and a RGB-D camera. These two simulated sensors have similar characteristics of the real ones, e.g. the camera has a restricted *field of view*.

Figure 4 depicts a typical simulation result with  $d = (0, 1)$  [m],  $(k_1, k_2, k_3, \varepsilon) = (1, 1, 1, 0.1)$  and the simulated person moved around an empty environment [13]. The trajectory of the person is illustrated in Figure 3 and is composed of four time intervals (see Figures 3 and 4):

- i)  $[0, t_A]$ : The person does not move, i.e.  $|v_p| = 0$ . Then, as expected, the control law (10) makes  $\tilde{p}_1$  to converge to zero, while the error  $\tilde{p}_2$  remains bounded (constant).
- ii)  $[t_A, t_B]$ : The person moves forward and then stops in **B**. Consequently, as long as the person moves,  $\tilde{p}_2$  tends to zero. When the person stops, i.e.  $|v_p| = 0$ ,  $\tilde{p}_2$  remains constant. Note that the angle  $\tilde{\theta}$  between the robot's axis  $\vec{i}$  and the velocity of the person  $\vec{v}_p$  converges to zero.
- iii)  $[t_B, t_C]$ : The person moves backward and then stops, for a little amount of time, in **C**. Note that the angle  $\tilde{\theta}$  tends

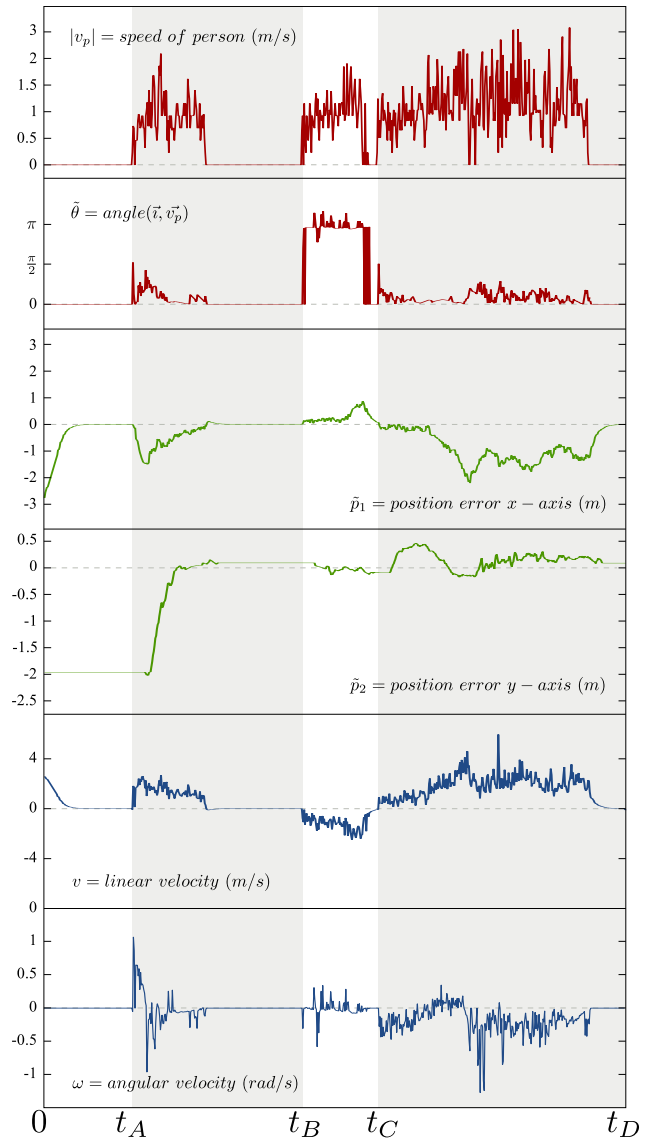


Fig. 4: Simulation results. From top to bottom, the speed of the person  $|v_p|$ , the angle  $\tilde{\theta}$ , the position errors  $\tilde{p}_1$  and  $\tilde{p}_2$ , and the control inputs  $v$  and  $\omega$  are depicted.

now to  $\pi$ , which means that the robot moves backward and does not turn round the person – *jack-knife effect* is avoided. The position errors are maintained *small*.

iv)  $[t_C, t_D]$ : The person starts moving forward and then performs a circular trajectory that ends in **D**. The robot control now minimizes  $\tilde{\theta} = 0$  and this means that the robot starts moving forward and then performs the circular trajectory. Still, position errors are kept *small*.

Encouraged by simulation results, we went one step further and carried out experiments with the aforementioned differential wheeled robot available at INRIA Sophia Antipolis. The control law (10) was evaluated with  $d = (0, 1.5)$  [m] and  $(k_1, k_2, k_3, \varepsilon) = (1, 0.1, 0.1, 0.1)$ , i.e. smaller gains than those used in simulations. This choice was made in order to obtain *smooth* robot behaviors at the expense of a degraded tracking quality. For instance, Figure 5, which

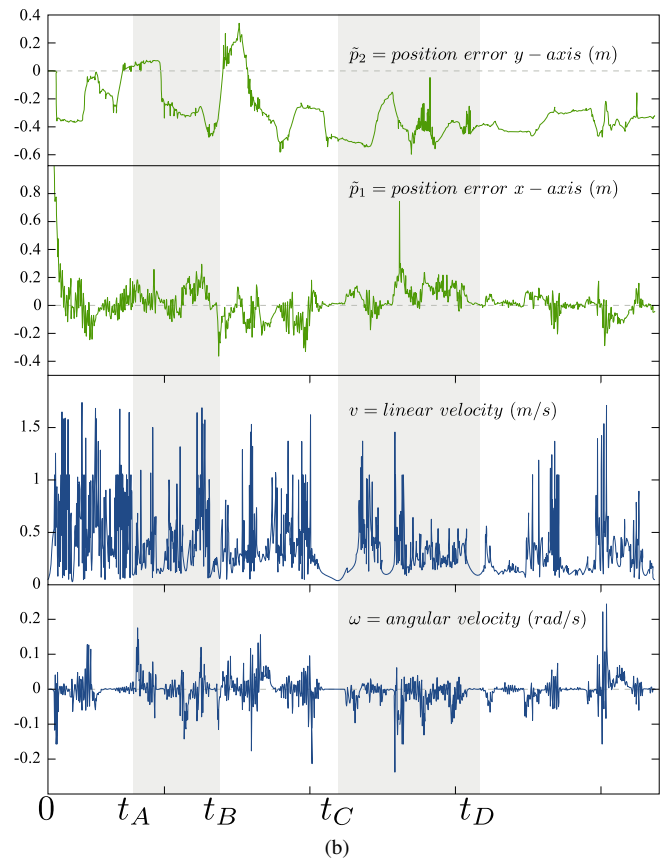
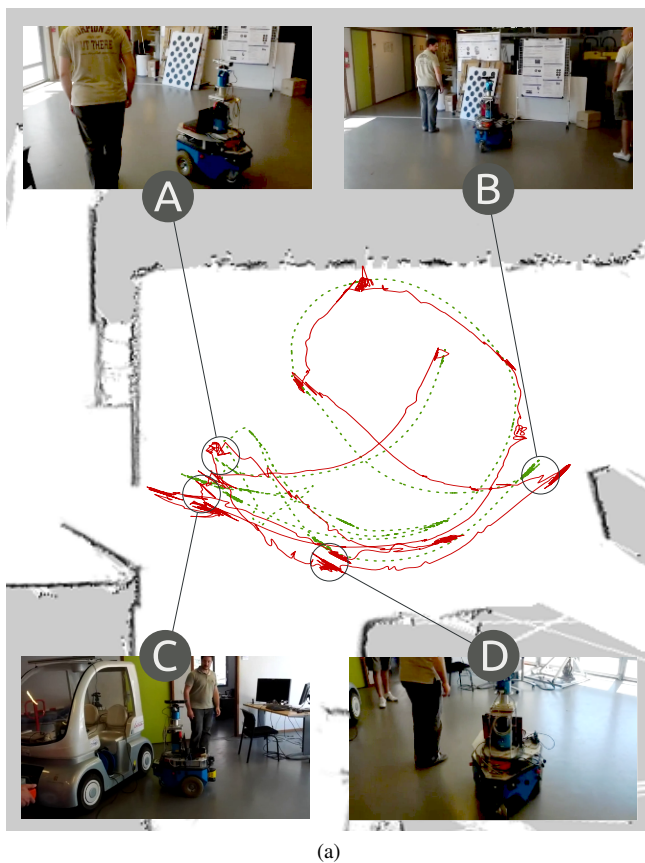


Fig. 5: Experimental results. From top to bottom, the position errors  $\tilde{p}_2$  and  $\tilde{p}_1$ , and the control inputs  $v$  and  $\omega$  are depicted.

depicts curves of a typical experimental result, shows that the position error  $\tilde{p}_2$  does not converge to zero, although maintained relatively *small*. This convergence is achieved for the component  $\tilde{p}_1$ . The fact that  $\tilde{p}_2$  does not converge to zero is basically due to three reasons: *i*) the velocity of the person was estimated from the measurement of its position under the assumption of *constant person velocity*, which is not the case; *ii*) the desingularized control law (10) neglects the *feed-forward* term  $\ddot{x}_p$ ; *iii*) measurement errors. Higher gains would improve the tracking quality in most cases, but measurement noise induces limitations on the values of these gains. Supplement material associated with this test is at

<http://goo.gl/NFnjg>

Let us remark that even during the experimental campaigns, the *jack-knife effect* is avoided – the robot moves according to the person’s direction of motion – although perfect tracking is not achieved.

## V. CONCLUSIONS

This article has presented a novel solution to the problem of person following for differential drive robots. The paper’s focus has been on control aspects. We have proposed control laws that ensure person following even when the user is located on the wheels’ axis, a situation where most classical control strategies developed so far fail. The present solution ensures jack-knife effect avoidance, which means that the

robot does not turn back when the user moves backward. This property could be useful for other applications. Then, simulations and experiments were carried out to verify the effectiveness of the proposed solution. The latter were performed with a differential drive robot equipped with two sensors: a laser range finder and a RGB-D camera. A data fusion algorithm was used to estimate the position of the user from the information provided by these two sensors.

We are aware that many issues need to be further investigated in the perspective of real-world applications to the person following problem. In particular, person recognition and position estimation, or obstacle avoidance, are fundamental issues that are only partially addressed in this paper. Further developments in this direction are necessary. Also, evaluating the tracking precision of the present control approach in relation to the person’s velocity is another important topic that must be further investigated.

## ACKNOWLEDGEMENTS

We are thankful to Patrick Rives and the Large Scale Initiative Action PAL (*Personally Assisted Living*), which funded this research, and to Glauco Scandaroli for the useful discussions during the development of this project.

## A. Proof of Theorem 1

The proof is based on a Lyapunov analysis. Consider the following candidate Lyapunov function:

$$V = \frac{1}{2}|\tilde{p}|^2 + \frac{1}{2k_2} \sin(\tilde{\theta})^2. \quad (11)$$

Define  $\xi := \text{atan2}(\dot{x}_{p2}, \dot{x}_{p1})$ . Then,  $\tilde{\theta} = \xi - \theta$ ,  $\dot{\theta} = \omega$ , and

$$\dot{\tilde{\theta}} = - \left( \omega + \frac{\dot{x}_p^T S \ddot{x}_p}{|\dot{x}_p|^2} \right). \quad (12)$$

Therefore  $\dot{V}$  along the solutions of System (7) is:

$$\begin{aligned} \dot{V} &= \tilde{p}_1 (v - d_2 \omega - v_{p1}) \\ &\quad - \frac{\sin(\tilde{\theta}) \cos(\tilde{\theta})}{k_2} \left[ \omega + \frac{\dot{x}_p^T S \ddot{x}_p}{|\dot{x}_p|^2} + \frac{k_2 \tilde{p}_2 |\dot{x}_p|}{\cos(\tilde{\theta})} \right]. \end{aligned}$$

By applying the control inputs  $(v, \omega)$  given by (9), the above expression of  $\dot{V}$  becomes:

$$\dot{V} = -k_1 \tilde{p}_1^2 - \frac{k_3}{k_2} \tan(\tilde{\theta})^2, \quad (13)$$

because

$$\frac{|\dot{x}_p|^2 v_{p2}}{v_{p1}^3} = \frac{\tan(\tilde{\theta})^2}{\sin(\tilde{\theta}) \cos(\tilde{\theta})}.$$

Since  $\dot{V}$  is negative semi definite, the system's trajectories are bounded. To claim that  $\dot{V} \rightarrow 0$ , we have to verify that  $\dot{V}$  is uniformly continuous, which is in turn implied by  $\dot{V}$  being bounded (LaSalle's Theorem does not apply since System (7) is time varying). Given (12), the time derivative of (13) is:

$$\ddot{V} = -2k_1 \tilde{p}_1 \dot{\tilde{p}}_1 + 2 \frac{k_3 \sin(\tilde{\theta})}{k_2 \cos(\tilde{\theta})^3} \left[ \omega + \frac{\dot{x}_p^T S \ddot{x}_p}{|\dot{x}_p|^2} \right]. \quad (14)$$

Since  $|\dot{x}_p| \neq 0 \forall t$  and the system's trajectories are bounded, then  $\dot{V}$  is bounded iff  $\tilde{\theta}$  never belongs to  $\{\frac{\pi}{2}, -\frac{\pi}{2}\}$ . To verify this condition, consider the following positive-definite function:

$$V_{\tilde{\theta}} = \frac{1}{2k_2} \sin(\tilde{\theta})^2, \quad (15)$$

whose time derivative along the solutions of System (12) with the control inputs given by (9) is:

$$\dot{V}_{\tilde{\theta}} = -\frac{k_3}{k_2} \tan(\tilde{\theta})^2 + \tilde{p}_2 v_{p2}. \quad (16)$$

Since the system's trajectories and the velocity  $\dot{x}_p$  are bounded, then there exists a constant  $c > 0$  such that:

$$\dot{V}_{\tilde{\theta}} < -\frac{k_3}{k_2} \tan(\tilde{\theta})^2 + c. \quad (17)$$

Therefore,  $\exists \varepsilon > 0$  such that if  $|\tilde{\theta} - \frac{\pi}{2}| < \varepsilon$ , then  $\dot{V}_{\tilde{\theta}} < 0$ . This in turn implies that  $\tilde{\theta}$  never crosses  $\frac{\pi}{2}$  because  $\theta = \frac{\pi}{2}$  is a local maximum of  $V$ . The fact that  $\tilde{\theta}$  never crosses  $\frac{3}{2}\pi$  can be proven analogously.

Consequently,  $\dot{V}$  is bounded  $\Rightarrow \dot{V}$  uniformly continuous  $\Rightarrow \dot{V} \rightarrow 0 \Rightarrow$

$$\tilde{p}_1 \rightarrow 0 \quad \text{and} \quad \tilde{\theta} \rightarrow \{0, \pi\}.$$

It is left to prove that  $\tilde{p}_2 \rightarrow 0$ . Define  $y \doteq \sin(\tilde{\theta})$ . Then  $\dot{y}(t)$  along the solutions of System (12) with the control inputs given by (9) is given by:

$$\dot{y}(t) = k_2 |\dot{x}_p| \tilde{p}_2 - k_3 \frac{\tan(\tilde{\theta})}{\cos(\tilde{\theta})}. \quad (18)$$

We know that  $y(t) \rightarrow 0$  because  $\tilde{\theta} \rightarrow \{0, \pi\}$ . In addition, since the system's trajectories are bounded,  $|\dot{x}_p| \neq 0 \forall t$ , and  $\tilde{\theta}$  never belongs to  $\{\frac{\pi}{2}, \frac{3}{2}\pi\}$ , then it is possible to verify that  $\dot{y}(t)$  is bounded, which implies  $\dot{y}(t) \rightarrow 0$ . Consequently,  $\tilde{p}_2 \rightarrow 0$  since  $|\dot{x}_p| \neq 0 \forall t$  and  $\tan(\tilde{\theta}) \rightarrow 0$  ( $\tilde{\theta} \rightarrow \{0, \pi\}$ ).

## REFERENCES

- [1] T. Fong, I. R. Nourbakhsh, Socially interactive robots, *Robotics and Autonomous Systems* 42 (3-4) (2003) 139–141.
- [2] L. M. Fuentes, S. A. Velastin, People tracking in surveillance applications, in: *In Proceedings of the 2nd IEEE International workshop on PETS*, 2001.
- [3] R. Bodor, B. Jackson, N. Papanikolopoulos, H. Tracking, Vision-based human tracking and activity recognition, in: *Proc. of the 11th Mediterranean Conf. on Control and Automation*, Kostrzewa Joseph, 2003, pp. 18–20.
- [4] J. Shotton, A. Fitzgibbon, M. Cook, T. Sharp, M. Finocchio, R. Moore, A. Kipman, A. Blake, Real-Time Human Pose Recognition in Parts from Single Depth Images, in: *Computer Vision and Pattern Recognition*, 2011. doi:10.1109/CVPR.2011.5995316.
- [5] A. Censi, An ICP variant using a point-to-line metric, in: *Proceedings of the IEEE International Conference on Robotics and Automation (ICRA)*, Pasadena, CA, 2008. doi:10.1109/ROBOT.2008.4543181.
- [6] K. O. Arras, S. Grzonka, M. Luber, W. Burgard, Efficient people tracking in laser range data using a multi-hypothesis leg-tracker with adaptive occlusion probabilities, in: *Proc. IEEE International Conference on Robotics and Automation (ICRA'08)*, Pasadena, USA, 2008.
- [7] T. Sonoura, T. Yoshimi, M. Nishiyama, H. Nakamoto, S. Tokura, N. Matsuhira, Person following robot with vision-based and sensor fusion tracking algorithm, in: *Computer Vision*, 2008. doi:DOI: 10.5772/6161.
- [8] M. Kristou, A. Ohya, S. Yuta, Target person identification and following based on omnidirectional camera and LRF sensor fusion from a moving robot, *Journal of Robotics and Mechatronics* 23 (1) (2011) 163.
- [9] G. Doisy, A. Jevtic, E. Lucet, Y. Edan, Adaptive person-following algorithm based on depth images and mapping, in: *Workshop on Robot Motion Planning: Online, Reactive, and in Real-time 2012 IEEE/RSJ International Conference on Intelligent Robots and Systems, IROS, Vilamoura, Portugal*, 2012.
- [10] P. Morin, C. Samson, *Handbook of Robotics*, Springer, 2008, Ch. Motion control of wheeled mobile robots, pp. 799–826.
- [11] H. Sidenbladh, D. Kragic, H. I. Christensen, A person following behaviour for a mobile robot, in: *ICRA*, 1999.
- [12] H. Takemura, N. Zentaro, H. Mizoguchi, Development of vision based person following module for mobile robots in/out door environment, in: *Proceedings of the 2009 international conference on Robotics and biomimetics, ROBIO'09*, IEEE Press, Piscataway, NJ, USA, 2009, pp. 1675–1680.
- [13] L. Marchetti, D. Pucci, P. Morin, Autonomous shopping cart platform for people with mobility impairments, in: *Proceedings of the IEEE/RSJ International Conference on Intelligent Robots and Systems (IROS)*, 2012.